Two-Dimensional Monte Carlo Simulations of Aggregation Phenomena in Ferromagnetic Colloidal Dispersions composed of Rod-like Hematite Particles

Akira Satoh*, Yasuhiro Sakuda and Yuta Katayama*****

* Faculty of System Science and Technology, Akita Prefectural University, 84-4, Ebinokuchi, Tsuchiya-aza, Yuri-honjo, Akita, 015-0055 Japan

** Graduate School of Akita Prefectural University, 84-4, Ebinokuchi, Tsuchiya-aza, Yuri-honjo, Akita, 015-0055 Japan

*** Ex-Graduate Student, Graduate School of Akita Prefectural University, 84-4, Ebinokuchi, Tsuchiya-aza, Yuri-honjo, Akita, 015-0055 Japan

*E-mail: asatoh@akita-pu.ac.jp

ABSTRACT

We have investigated aggregation phenomena of ferromagnetic colloidal dispersions composed of rod-like hematite particles which have a magnetic moment normal to the particle axis, by means of the cluster-moving Monte Carlo method. In concrete, we have treated a two-dimensional dispersion in order to clarify the influences of the particle aspect ratio, magnetic interactions between particles and the magnetic field strength on particle aggregations. The main results obtained here are summarized as follows. In the absence of an applied magnetic field, rod-like particles tend to aggregate to form raft-like clusters along the magnetic moment direction as magnetic particle-particle interactions increase. However, shorter raft-like clusters are formed as the area fraction decreases. If a strong magnetic field is applied, the raft-like clusters tend to incline along the magnetic field direction, and this feature of the cluster formation is not significantly dependent on the particle length.

Keyword: Ferromagnetic Colloidal Dispersion, Aggregation Phenomena, Rod-like Particle, Raft-like Cluster, Pair Correlation Function, Orientational Pair Correlation Function

NOMENCLATURE

d	=	diameter of spherical particles in a rod-like hematite particle
$\boldsymbol{e}_{m_i}$	=	unit vector along the magnetic moment vector $\boldsymbol{m}_i$
$\boldsymbol{H}$	=	external magnetic field
H	=	magnitude of the external magnetic field
k	=	Boltzmann's constant
L	=	unit cell length
$\boldsymbol{m}_i$	=	magnetic moment vector of particle i
m	=	magnitude of the magnetic moment vector $\boldsymbol{m}_i$
n	=	number density of particles
N	=	total number of particles
N_P	=	number of constituent particles
N_S	=	number of clusters
n_s	=	number density of surfactant molecules on a particle surface
r_{coff}	=	cutoff distance
$\boldsymbol{r}_i$	=	position vector of particle i
$\boldsymbol{r}_{ij}$	=	vector drawn from particles j to i
r_{ij}	=	magnitude of the vector $\boldsymbol{r}_{ij}$

S = number of constituent particles
T = temperature of a carrier liquid
$\boldsymbol{t}_{ij}$ = unit vector along the vector $\boldsymbol{r}_{ij}$
t_δ = ratio of the thickness of the surfactant layer , δ, to the radius of the solid part of a particle, $d/2$
$u_i^{(H)}$ = interaction energy of magnetic dipole-field interaction
$u_{ij}^{(m)}$ = interaction energy of magnetic dipole-dipole interaction
$u_{ij}^{(v)}$ = interaction energy arising due to overlapping of the surfactant layers
δ = thickness of the surfactant layer
θ = angle from the x-axis direction for the pair correlation function
ψ_{ij} = angle between two axes of particles i and j
λ = dimensionless parameter representing the strength of magnetic particle-particle interactions
λ_v = dimensionless parameter representing the strength of steric interactions between two spherical particles with diameter d
μ_0 = permeability of free space
ξ = dimensionless parameter representing the strength of particle-field interactions
ϕ_a = area fraction of particles

1. INTRODUCTION

New functional materials may be developed by controlling microstructures artificially for exhibiting desired functional properties. Suspensions composed of functional particles have a significant possibility for generating such materials. For example, if magnetic rod-like particles are sedimented under circumstances of the gravity field, the particle orientational distribution is controlled by an applied magnetic field, and the base liquid is evaporated, then we can obtain high-density magnetic recording materials (tapes) [1,2]. In this example, a suspension composed of magnetic rod-like particles appears as a transient medium for developing a final functional material. Furthermore, self-organization structures of magnetic rod-like particles in such suspensions may lead to a functional fluid with significant magneto-rheological effects. In this example, magneto-rheological effects are controlled by changing internal structures of magnetic rod-like particles using an applied magnetic field, and these magneto-rheological effects are used for developing mechanical dampers and actuators [3]. In the fields such as the colloid physics engineering, the following applications are under being developed: for examples, three-dimensional photonics crystal for application to light units [4-6], extension of such colloid crystals to laser emission [7,8], etc.

Typical functional fluids are magneto-rheological fluids and magnetic fluids (ferrofluids), which are suspensions composed of magnetic spherical particles. Our research group, therefore, has been conducting a series of studies concerning aggregation phenomena by means of molecular simulation methods. For example, Monte Carlo (MC) simulations for a mono-disperse system [9,10], and for a poly-disperse system [11,12]. In these works, it has been clarified that thick chainlike clusters are formed in the magnetic field direction. The shape of magnetic particles is another governing factor, besides magnetic particle-particle interactions, for determining the microstructures of a suspension. Hence, Monte Carlo simulations of colloidal dispersions composed of magnetic rod-like particles with a magnetic moment along the particle axis have been conducted in thermodynamic equilibrium for various particle aspect ratios [13,14]. These works show that various microstructures such as raft-like and anti-parallel structures are formed, depending on the particle aspect ratio.

Different types of magnetic rod-like particles are also attractive from an application point of view. A suspension composed of hematite particles with a magnetic moment normal to the particle axis was synthesized by Ozaki et al. [15,16]. Several theoretical works for this suspension show that the rod-like particle can rotate freely to a certain degree with the magnetic moment remaining inclining in the magnetic field direction under a simple shear flow [17,18]. This behavior is completely different from a suspension composed of rod-like particles magnetized in the particle axis. In addition, the control of the orientational distribution of such particles on the surface of materials may lead to the development of a new surface-quality-changing technology such as capsules, including cancer medicines inside, coated with magnetic fine particles. In this case, a two-dimensional system of a magnetic dispersion has to be treated in order to investigate aggregation phenomena.

In the present study, therefore, we attempt to clarify the influences of the particle length (or aspect ratio), area fraction, magnetic particle-particle and particle-field interactions, etc., on aggregation phenomena, by means of the cluster-moving Monte Carlo simulations. To do so, we treat a two-

dimensional system composed of rod-like particles with a magnetic moment normal to the particle axis. Snapshots, orientational pair correlation functions and number distributions of clusters are used for discussing the results qualitatively and quantitatively.

2. PARTICLE MODEL

As shown in Figure 1, the experimental observation shows that rod-like hematite particles have a shape of spheroid [15,16]: (*l, d*) in Figure 1 is the lengths of the major and minor axes of the particle. However, spheroidal particles are difficult in determining whether or not particles overlap in a simulation procedure, so that we use a simple particle model such as a sphere-connected model, shown in Figure 2. In this particle model, a rod-like particle is modeled as N_P spheres connected linearly. The length of the rod-like particle is expressed by the number of constituent particles, N_P. Such a sphere-connected particle is covered with a surfactant layer (steric layer) with a constant thickness δ. If the center-to-center distance for particles i and j is denoted by r_{ij}, the magnetic moment of particle i by $\boldsymbol{m}_i$, and the magnetic field by $\boldsymbol{H}$ (H=|$\boldsymbol{H}$|), then the interaction energy of particle i with the magnetic field, $u_i^{(H)}$, and the interaction energy between particles i and j, $u_{ij}^{(m)}$, are expressed, respectively, as [19]

$$u_i^{(H)} = -kT\xi \boldsymbol{e}_{m_i} \cdot \boldsymbol{H} / H \tag{1}$$

$$u_{ij}^{(m)} = kT\lambda \frac{d^3}{r_{ij}^3}\left\{ \boldsymbol{e}_{m_i} \cdot \boldsymbol{e}_{m_j} - 3(\boldsymbol{e}_{m_i} \cdot \boldsymbol{t}_{ij})(\boldsymbol{e}_{m_j} \cdot \boldsymbol{t}_{ij}) \right\} \tag{2}$$

in which ξ and λ are the non-dimensional parameters representing the strengths of particle-field and particle-particle interactions, respectively. These expressions are as follows:

$$\xi = \mu_0 mH / kT\,, \quad \lambda = \mu_0 m^2 / 4\pi d^3 kT \tag{3}$$

in which k is Boltzmann's constant, T is the temperature, μ_0 is the permeability of free space, m (= |$\boldsymbol{m}_i$|) is the magnitude of magnetic moment, $\boldsymbol{e}_{m_i}$ and $\boldsymbol{t}_{ij}$ are unit vectors, expressed as $\boldsymbol{e}_{m_i} = \boldsymbol{m}_i/m$ and $\boldsymbol{t}_{ij} = \boldsymbol{r}_{ij}/r_{ij}$, d is the diameter of constituent particles, and δ is the thickness of the steric layer.

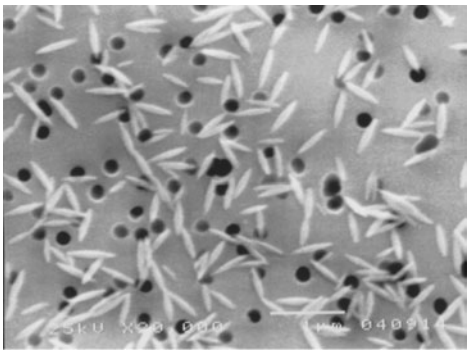

Figure 1. Electron microscopy image of a hematite particle dispersion ((*l*,*d*)=(0.45±0.05, 0.09±0.01) μm).

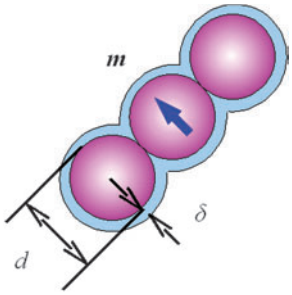

Figure 2. Rod-like hematite particle model composed of connected spherical particles covered with a steric layer for N_P = 3

When particles approach each other and the steric layers overlap, the repulsive interaction comes to arise. The expression for this interaction energy is written as [19]

$$u_{ij}^{(v)} = kT\lambda_v \left(2 - \frac{2r_{ij}/d}{t_\delta} \ln\left(\frac{d+2\delta}{r_{ij}} \right) - 2\frac{r_{ij}/d - 1}{t_\delta} \right) \tag{4}$$

in which t_δ is the ratio of the thickness of the steric layer to the particle radius, that is, $t_\delta = 2\delta/d$. The notation λ_v is the non-dimensional parameter representing the strength of the interaction due to the overlapping of steric layers, expressed as $\lambda_v = \pi d^2 n_s/2$, in which n_s is the number of surfactant molecules per unit area on the surface of the spherical particles.

3. CLUSTER-MOVING MONTE CARLO METHOD

For a strongly interacting system, the ordinary Metropolis Monte Carlo method cannot capture a physically reasonable cluster formation. After particles combine with each other, such combined particles cannot dissociate in a strongly-interacting system. This means that the convergence to equilibrium state is extraordinary slow for usual Monte Carlo simulations.

In the cluster-moving Monte Carlo method [21], clusters which are formed during the process of a simulation run are moved as unitary particles. This procedure leads to the acceleration of the particle aggregation process, so that the present study uses this cluster-moving Monte Carlo method. The main part of the cluster-moving algorithm, that is, the transition from states i to j, is written as

a. Check the formation of clusters
b. Select a cluster
c. Compute the interaction energy of the selected cluster with the other clusters, U
d. Move the cluster randomly and compute the interaction energy of the cluster at the new position, U'
e. If $\Delta U = U' - U \le 0$, then accept the new position and return to step b
f. If $\Delta U > 0$, then generate a uniform random number R ($0<R<1$)
   f.1 If $\exp(-\Delta U/kT) \ge R$, then accept the new position and return to step b
   f.2 If $\exp(-\Delta U/kT) < R$, then reject the movement, retain the old position, and return to step b (the old state is regarded as a new state for averaging procedures)

4. QUANTITATIVE EVALUATION OF AGGREGATE STRUCTURES

In order to evaluate the internal structures of aggregates, we use the pair correlation function $g^{(2)}(r^*,\theta)$, orientational pair correlation function $g_{ori}^{(2)}(r^*)$, and radial distribution function $g(r^*)$, in which r^* ($=r/d$) is the dimensionless radial distance from the particle of interest, and θ is the angle from the x-axis direction. The pair correlation and radial distribution functions are defined in a usual manner, and the orientational pair correlation function is defined as

$$g_{ori}^{(2)}(r^*) = \frac{\dfrac{1}{nN}\left\langle \sum_i \sum_{\substack{j \\ (i\neq j)}} P_2(\cos\psi_{ij})\,\delta(\boldsymbol{r}_{ij}^{\,*} - \boldsymbol{r}^*) \right\rangle}{\dfrac{1}{nN}\left\langle \sum_i \sum_{\substack{j \\ (i\neq j)}} \delta(\boldsymbol{r}_{ij}^{\,*} - \boldsymbol{r}^*) \right\rangle} \tag{5}$$

in which ψ_{ij} is the angle between the particle axis directions of particles i and j, $P_2(\cos\psi_{ij})$ is the Legendre function, defined as $P_2(\cos\psi_{ij}) = (3\cos^2\psi_{ij} - 1)/2$, N is the number of particles, n is the number density, and $\boldsymbol{r}^*$ is the dimensionless position vector, expressed as $\boldsymbol{r}^* = \boldsymbol{r}/d$.

In two-dimensional simulations, the orientational pair correlation function was evaluated by the following expression:

$$g_{ori}^{(2)}(r^*) = \frac{1}{n^* g(r^*)} \cdot \frac{1}{N} \left\langle \sum_{i=1}^{N} \frac{\sum' P_2(\cos\psi_{ij})}{2\pi r^* \Delta r^*} \right\rangle \tag{6}$$

in which Σ' means the summation concerning all particles which are located within a small area $2\pi r^*\Delta r^*$, and n^* is the dimensionless number density, expressed as $n^*=nd^3$. The expressions for $g^{(2)}(r^*,\theta)$ and $g(r^*)$ are written in the literature [19,20].

5. PARAMETERS FOR SIMULATIONS

The simulation region is taken as a square with a length $L^*(=L/d)$, and the usual periodic boundary condition is used. Particles are initially located on each site of the square lattice, and the particle orientation is randomly given. The following conditions were used in simulations. The two-dimensional system is treated, and the number of particles is taken as N=1024. The non-dimensional parameter λ_v is 150, and the thickness of steric layer δ is 0.15d. The distance for judging the cluster formation is taken as r_c=1.2d, and the cut-off distance r_{coff} is 10d. The maximum distance and angle for the translational and rotational motion are 0.5d and 5°, respectively. Under the above-mentioned conditions, simulations were carried out for various cases of parameters. The area fraction ϕ_a, which is defined using the solid part of particles and expressed as $\phi_a = \pi N_P N/4L^{*2}$, is taken as $\phi_a = 0.05$, 0.1 and 0.2, and the number of constituent particles (the length of rod-like particles), N_P, is 3, 5 and 7. Also, the non-dimensional parameters representing the strength of particle-field and particle-particle interactions, ξ and λ, are taken as $\xi = 0$, 1, 5, 10 and 20, and $\lambda = 1$, 10 and 20. The cluster-moving procedure was carried out every 10 MC steps, and continued until 200,000 MC steps. After that, another 1,000,000 MC steps were conducted without the cluster-moving procedure. The quantities of interest were evaluated using the data which were obtained within the last 700,000 MC steps.

In a strongly-interacting system of magnetic spherical particles, the cluster-moving method has been clarified to be indispensable [21], since magnetic particles cannot dissociate from their cluster to join in other glowing clusters, which may lead to the formation of long chain-like clusters, in the usual Metropolis algorithm. However, for the present rod-like particle system, they have the rotational motion to change their positions and can combine with glowing clusters, almost independently of the translational motion. Hence, it is noted that the present results obtained by the cluster-moving method are not significantly different from those obtained by the usual Metropolis MC algorithm.

6. RESULTS AND DISCUSSION

6.1 No Applied Magnetic Field Case

6.1.1 Influences of magnetic particle-particle interactions

As already pointed out in Introduction, we here concentrate our attention on aggregation phenomena in a two-dimensional system, since the control of the orientational distribution of rod-like particles on the material surface has to be clarified to develop a new surface-quality-changing technology. In the following, we discuss the influences of magnetic interactions between particles on aggregation phenomena in terms of snapshots and the orientational pair correlation function.

Figure 3 shows snapshots for the particle length $N_P = 3$ and the area fraction $\phi_a = 0.2$: Figures 3(a) and 3(b) are for $\lambda = 5$ and 10, respectively. It is seen from Figure 3(a) that many rod-like particles move

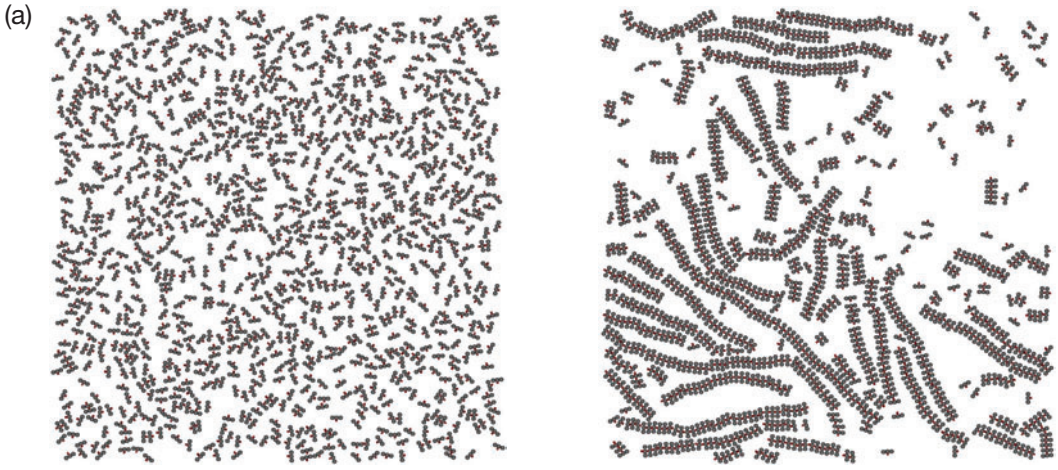

Figure 3. Influences of magnetic particle-particle interactions on aggregate structures for $N_P = 3$ and $\phi_a = 0.2$: (a) $\lambda = 5$; (b) $\lambda = 10$

separately without significant aggregation. This is mainly because the magnetic interactions between particles are not significantly strong for the formation of clusters, although several short clusters composed of two or three particles are observed. On the other hand, many long raft-like clusters are observed in Figure 3(b) for $\lambda = 10$. In this case, the magnetic interactions between particles are sufficiently strong, so that they promote short raft-like clusters to aggregate to form long clusters. These long raft-like clusters are not so linear, but relatively bent.

Now, we discuss the internal structures of clusters quantitatively in terms of the orientational pair correlation function. Figure 4 shows the results of such an orientational pair correlation function for $N_P = 3$ and $\phi_a = 0.2$: three cases are shown in Figure 4 for $\lambda = 5$, 10 and 20. The abscissa is the radial center-to-center distance between rod-like particles and the ordinate stands for the correlation of the orientation of two particles. It is noted that, when $g_{ori}^{(2)}(r^*) = 1$, two rod-like particles incline in a parallel way, when $g_{ori}^{(2)}(r^*) = 0$, they incline randomly without any correlation, and, for the case of $g_{ori}^{(2)}(r^*) = -0.5$, they incline perpendicularly.

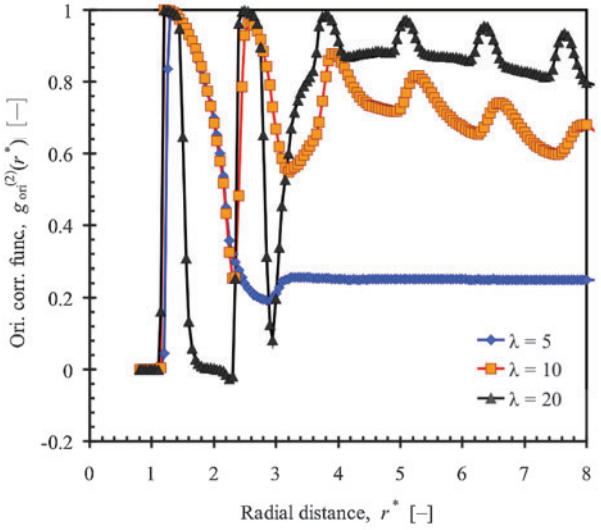

Figure 4. Influences of magnetic particle-particle interactions on orientational pair correlation functions for $N_P = 3$ and $\phi_a = 0.2$

For λ=5, one significant peak alone is observed at $r^* \approx 1.3$, which clearly shows the characteristic property that many short raft-like clusters are formed in Figure 3(a). For λ=10, the curve changes significantly and converges to a certain value with increasing the radial distance. It is seen that the peaks appear at positions of integer times $(1+t_\delta)d$, which means that the rod-like particles aggregate to form raft-like clusters with almost pointing to the same direction, and this property remains in a long range way.

For $\lambda = 20$, significant correlation remains in a long range area, but the peaks arise at relatively shorter positions of integer times $(1 + t_\delta)d$. This implies that the steric layers of the particles overlap, since magnetic interactions between particles are significantly larger than the thermal energy. Additionally, regular peaks appearing in a long range area means that significantly long raft-like clusters are formed. We may conclude from the above discussion that the raft-like clusters become longer with increased values of the magnetic particle-particle interactions.

6.1.2 Influences of area fraction

We discuss the influences of the area fraction of particles on aggregation phenomena in terms of snapshots, orientational pair correlation functions, and number distributions of clusters.

Figure 5 shows snapshots for $N_P = 3$ and $\lambda = 10$: Figures 5(a) and 5(b) are for $\phi_a = 0.1$ and 0.05, respectively. As already shown, many longer clusters are observed for =0.2 (in Figure 3(b)), but, in the case of $\phi_a = 0.1$ (in Figure 5(a)), relatively short clusters alone are formed. As the area fraction decreases such as $\phi_a = 0.05$, more particles come to move individually without significant aggregation. That is, raft-like clusters become shorter with the decrease in the area fraction. This is mainly because the opportunity of meeting each other due to magnetic particle-particle interactions decreases; more space is given to each particle with the decrease in the area fraction.

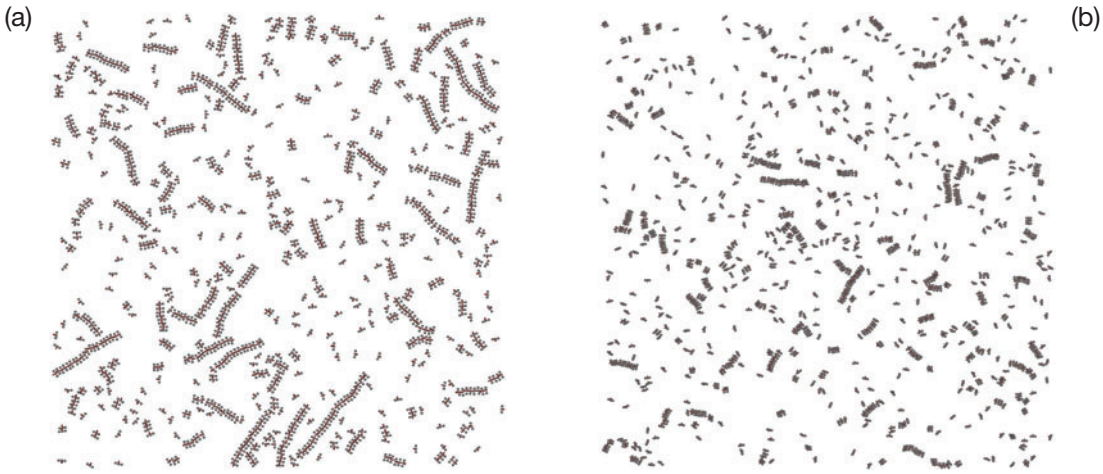

Figure 5. Influences of area fraction ϕ_a on aggregate structures for N_P = 3 and λ = 10: (a) ϕ_a = 0.1; (b) ϕ_a = 0.05

Figure 6 shows the number distribution of clusters: the abscissa S is the number of constituent particles of a cluster (corresponding to the cluster length), and the ordinate N_S is the ensemble average of the number of clusters composed of S particles. For any cases of ϕ_a, the number of clusters decreases with values of S, but characteristics of N_S at large values of S have to be focused on more carefully. For ϕ_a = 0.2, lager values remain significantly with increasing S, compared with the other cases, which clearly shows that there are many longer raft-like clusters in a system. For ϕ_a = 0.1, large clusters with the size over S≈30 significantly decrease compared with the case of ϕ_a = 0.2. For ϕ_a = 0.05, the system is relatively dilute, so that there are many short clusters without significant aggregation. These characteristics of the number distribution of clusters clearly explain those of the aggregate structures shown in Figure 5 as snapshots.

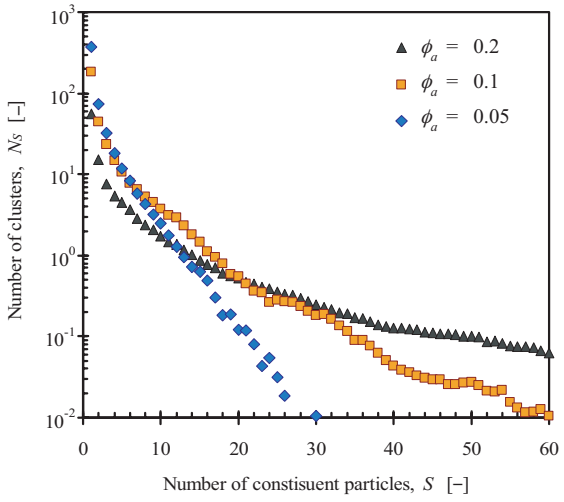

Figure 6. Influences of area fraction on number distributions of clusters for each size cluster in the case of N_P = 3 and λ = 10

Figure 7 shows the results of the orientational pair correlation function for three cases of the area fraction, ϕ_a = 0.2, 0.1 and 0.05; the result for ϕ_a = 0.2 has already been shown in Figure 4. For any cases of ϕ_a, peaks appear at positions of integer times $(1 + t_\delta)d$, which is in quite contrast with the results shown in Figure 4. This shows that the distance between the neighboring particles are dependent on values of λ, not on the area fraction. Although the characteristic of the correlation is not different within the short range for any cases, this property decreases more significantly for smaller values of ϕ_a. This corresponds to many shorter clusters formed with decreasing the area fraction, as shown in Figure 5.

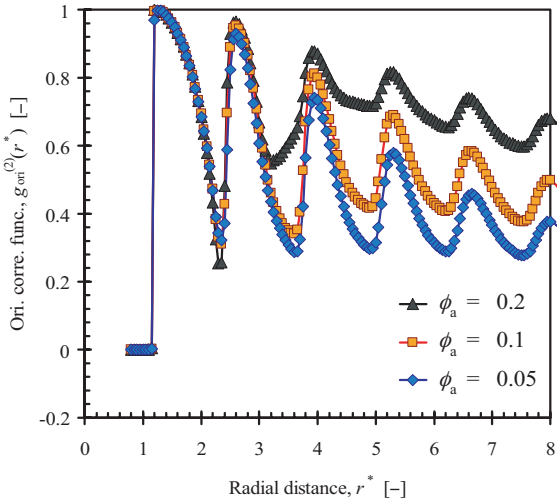

Figure 7. Influences of area fraction on orientational pair correlation functions for $N_P = 3$ and $\lambda = 10$

6.1.3 Influences of the particle length

The dependence of the aggregate structures on the particle length is discussed in the following. Figure 8 shows the snapshots for $\lambda = 10$ and $\phi_a = 0.2$: Figures 8(a) and 8(b) are for the particle size of $N_P = 5$ and 7, respectively. It is seen from comparing these snapshots with that in Figure 3(b) that shorter raft-like clusters are observed, and more single-moving particles remain for the case of longer particles. These characteristics may be explained in the following. The longer the particle becomes, the more strictly the particle rotational motion is restricted, which disturbs the growth of the cluster formation. These characteristics may be explained quantitatively more clearly using the cluster size distributions. Figure 9 shows the results of the number of clusters as a function of the number of constituent particles for N_P = 3, 5 and 7. It is clearly seen from Figure 9 that longer raft-like clusters are formed more significantly as the particle length N_P decreases.

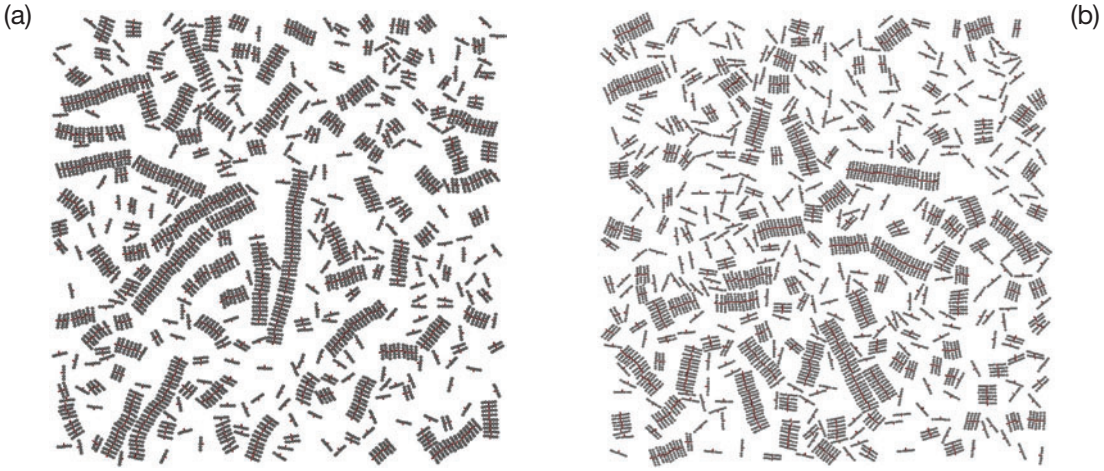

Figure 8. Influences of particle length N_p on aggregate structures for $\phi_a = 0.2$ and $\lambda = 10$: (a) $N_p = 5$; (b) $N_p = 7$

6.2 Applied Magnetic Field Case

6.2.1 Influences of magnetic particle-particle interactions

Finally, we discuss aggregation phenomena under circumstances of an applied magnetic field. Figure 10 shows snapshots for $N_P = 3$ and $\phi_a = 0.2$, and for a strong magnetic field case such as $\xi = 20$: Figures 10(a) and 10(b) are for λ = 5 and 10, respectively, and the magnetic field is applied in the upper direction of the paper. Although almost all particles move separately in Figure 3(a), a strong external

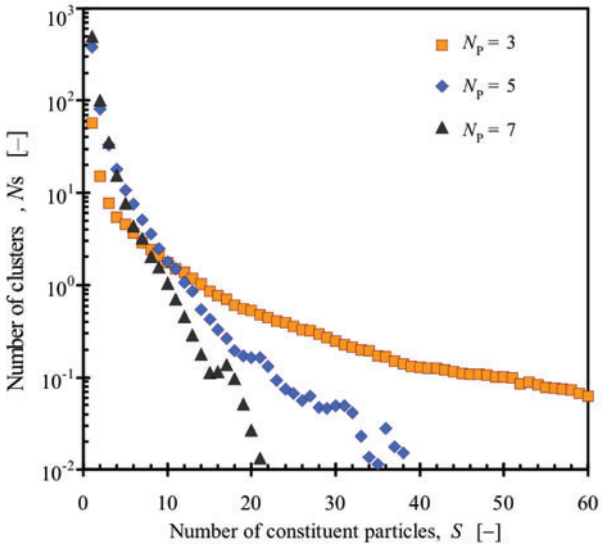

Figure 9. Influences of particle length N_P on number distributions of clusters for each size cluster in the case of $\phi_a = 0.2$ and $\lambda = 10$

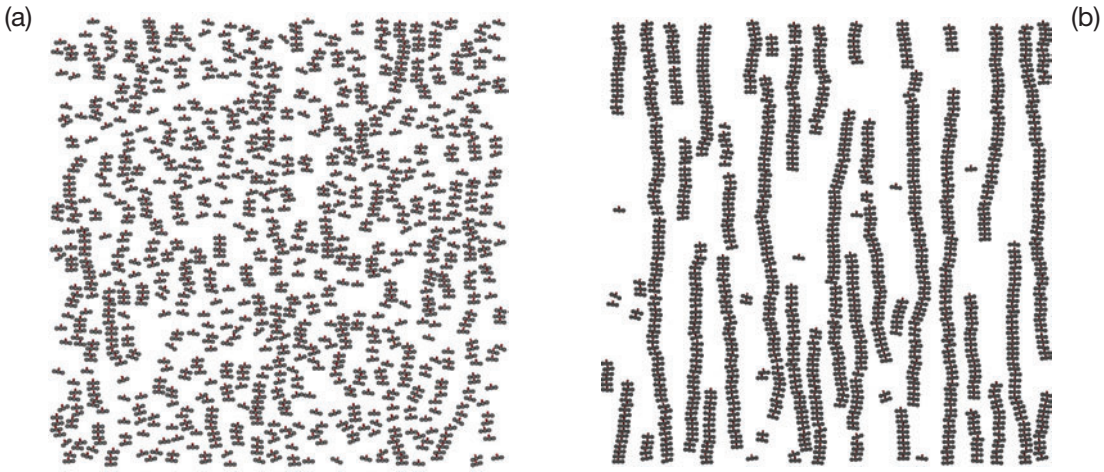

Figure 10. Influences of magnetic particle-particle interactions on aggregate structures for $\xi = 20$, $N_P = 3$ and $\phi_a = 0.2$: (a) $\lambda = 5$; (b) $\lambda = 10$

field enhances the cluster formation along the field direction (in Figure 10(a)). This is because the magnetic moment of each particle has a significant tendency to incline in the field direction under a strong external magnetic field, and this inclination of the magnetic moments induces the particle aggregation along the field direction. For strong magnetic particle-particle interactions such as $\lambda = 10$ (in Figure 10(b)), these magnetic interactions enhance such cluster formation more significantly, and many long raft-like clusters come to be formed along the field direction. However, it is not observed in Figure 10(b) that such long raft-like clusters aggregate to form thicker column-like clusters, which is in significant contrast with a spherical particle system [9,10]; thick chain-like clusters are formed for relatively strong magnetic interactions in this system.

Figure 11 shows the pair correlation function along the field direction, $g_{\parallel}^{(2)}(r^*)(= g^{(2)}(r^*, 90^\circ))$; the magnetic field is applied in the direction of $\theta = 90°$. For $\lambda = 5$, the correlation exists in a short range and is liquid-like, so that many short clusters observed in Figure 10(a) are not so stable and are expected to dissociate and associate repeatedly. The curves for $\lambda = 10$ and 20 exhibit that raft-like clusters are solid-like and quite stable without dissociations. As already pointed out, stronger magnetic interactions induce more significant particle overlapping, so that each peak for $\lambda = 20$ arises at positions shorter than integer times $(1+ t_\delta)d$.

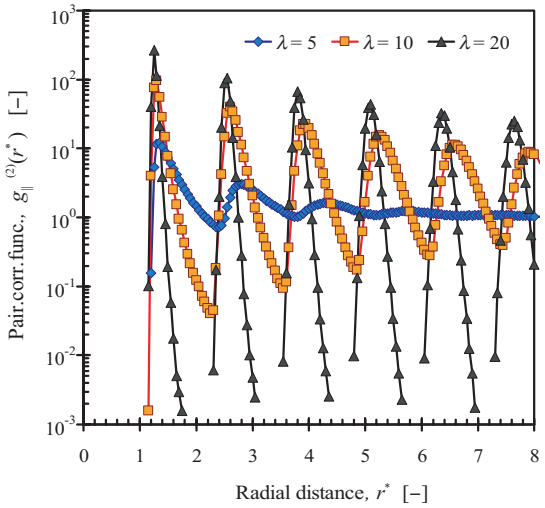

Figure 11. Influences of magnetic particle-particle interactions on pair correlation functions along the magnetic field for $\xi = 20$, $N_P = 3$ and $\phi_a = 0.2$

6.2.2 Influences of the particle length

Figure 12 shows snapshots for $\xi = 20$, $\lambda = 10$ and $\phi_a = 0.2$: Figures 12(a) and 12(b) are for the cluster size of $N_P = 5$ and 7, respectively. In the case of no external field (in Figure 8), the length of raft-like clusters is significantly dependent on the particle size N_P, but, in the present case a strong magnetic field, the cluster length seems to be not so different in the two cases of $N_P = 5$ and 7. This suggestion is supported by the results of the cluster size distribution shown in Figure 13. The curve of $N_P = 7$ in Figure 13 almost coincides with that for $N_P = 5$. Even the curve for $N_P = 3$ does not deviate significantly from the other two curves. These characteristics are in significant contrast with the previous results shown in Figure 6, and are explained in the following. In the case of no external magnetic field, the growth of raft-like clusters does not have a specific favored direction, so that the freedom of the rotational motion of clusters has a significant influence on the cluster size (or length); raft-like clusters cannot grow unless sufficient space exists, and such free space becomes smaller for larger particles. In contrast, for a strong magnetic field, free space for the growth of clusters is almost independent of the particle size, because the raft-like clusters strongly tend to incline in the field direction and do not need to rotate for growing to form longer raft-like clusters.

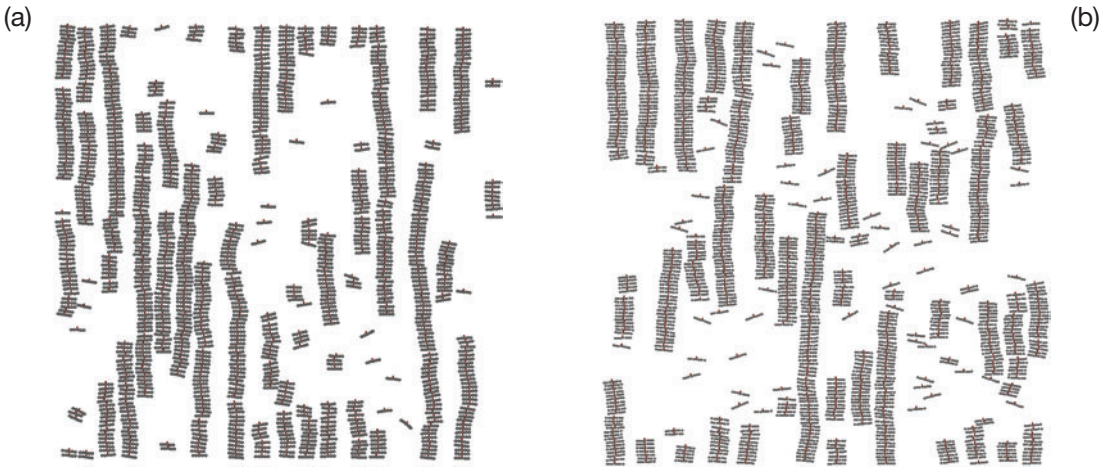

Figure 12. Influences of particle length N_P on aggregate structures for $\xi = 20$, $\lambda = 10$ and $\phi_a = 0.2$: (a) $N_P = 5$; (b) $N_P = 7$

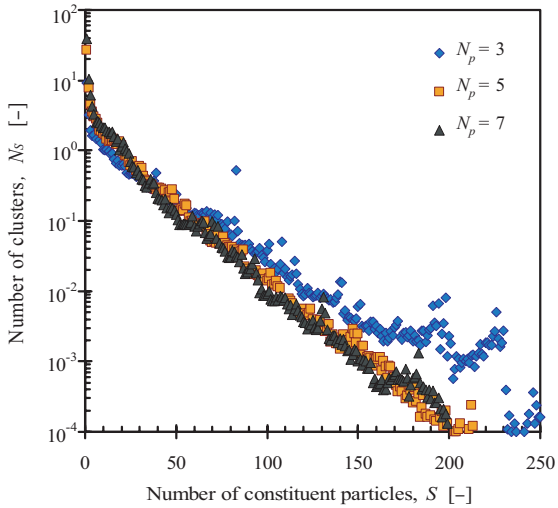

Figure 13. Influences of particle length on number distributions of clusters for each size cluster in the case of $\xi = 20$, $\lambda = 10$ and $\phi_a = 0.2$

Finally, we see the results of the pair correlation function along the magnetic field direction, which is shown in Figure 14. It is clearly seen from Figure 14 that the curve of $g_{\parallel}^{(2)}(r^*)$ as a function of the radial distance is almost in good agreement among three cases, which means that the internal structures of the raft-like clusters shown in Figures 12(a) and 12(b) are almost independent of the particle size N_P. One minor different point is that each peak for $N_P = 3$ appears at positions slightly shorter than those for $N_P = 5$ and 7. This is because a small angle change in the particle orientation has a slightly more influence on the internal structures of raft-like clusters for longer particle cases; that is, slightly more space arises between the neighboring particles in a cluster for longer particles.

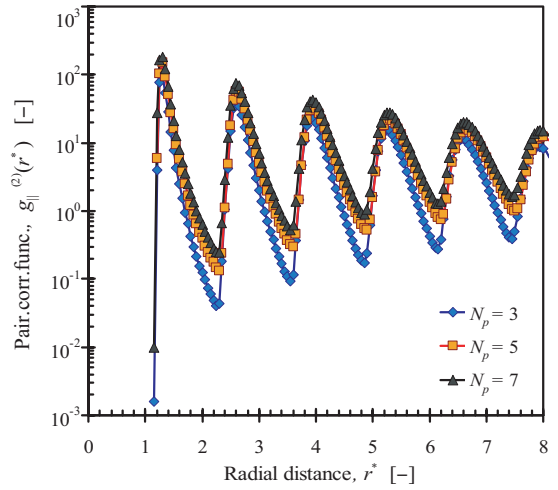

Figure 14. Influences of particle length on pair correlation functions along the magnetic field for $\xi = 20$, $\lambda = 10$ and $\phi_a = 0.2$

7. CONCLUSION

We have investigated aggregation phenomena of a ferromagnetic colloidal dispersion composed of rod-like hematite particles with a magnetic moment normal to the particle axis, by means of the cluster-moving Monte Carlo method. In concrete, we have treated a two-dimensional mono-dispersed model system in order to clarify the influences of the particle length, area fraction of particles, magnetic interactions between particles and the magnetic field strength on particle aggregation phenomena. Internal microstructures of the aggregates have been discussed quantitatively in terms of radial

distribution, pair correlation, orientational pair correlation functions, and number distributions of clusters. The main results obtained here are summarized as follows. In the absence of an applied magnetic field, rod-like particles tend to aggregate to form raft-like clusters along the magnetic moment direction as magnetic particle-particle interactions increase. However, shorter raft-like clusters are formed as the area fraction decreases. If a strong magnetic field is applied, the raft-like clusters tend to incline along the magnetic field direction, and this feature of the cluster formation is not significantly dependent on the particle length.

REFERENCES

[1] Verdes, C., Chantrell, R.W., Satoh, A., Harrell, J.W. and Nikles, D.E., Self-Organisation, Orientation and Magnetic Properties of FePt Nanoparticle Arrays, *J. Mag. Mag. Mater.*, 2006, 304, 27-31.

[2] Harrell, J.W., Kang. S., Jia, Z., Nikles, D.E., Chantrell, R.W. and Satoh, A., A Model for the Easy-Axis Alignment of Chemically Synthesized $L1_0$ FePt Nanoparticles, *Appl. Phys. Lett.*, 2005, 202508.

[3] Bullough, W.A., ed., Electro-Rheological Fluids, *Magneto-Rheological Suspensions and Associated Technology*, World Scientific, Singapore, 1996.

[4] Reese, C.E., Guerrero, C.D., Weissman, J.M., Lee, K. and Asher, S.A., Synthesis of Highly Charged, Monodisperse Polystyrene Colloidal Particles for the Fabrication of Photonic Crystals, *J. Colloid. Inter. Sci.*, 2000, 232, 76-80.

[5] Iwayama Y., Yamanaka, J., Takiguchi, Y., Takasaka, M., Itoh, K., Shinohara, T., Sawada, T. and Yonese, M., Optically Tunable Gelled Photonic Crystal Covering Almost the Entire Visible Light Wavelength Region, *Langmuir*, 2003, 19(4), 977-980.

[6] Mine E., Hirose, M., Nagao, D., Kobayashi, Y. and Konno, M., Synthesis of Submicron-Sized Titania Spherical Particles with a Sol-Gel Method and Their Application to Colloidal Photonic Crystals, *J. Colloid. Inter. Sci.*, 2005, 291, 162-168.

[7] Furumi, S. and Sakka, Y., Chiroptical Properties Induced in Chiral Photonic-Bandgap Liquid Crystals Leading to a Highly Efficient Laser-Feedback Effect, *Adv. Mater.*, 2006, 18, 775-780.

[8] Furumi, S. and Sakka, Y., Circularly Polarized Laser Emission Induced by Supramolecular Chirality in Cholesteric Liquid Crystals, *J. Nanosci. Nanotech.*, 2006, 6, 1819-1822

[9] Satoh, A., Chantrell, R.W., Kamiyama, S. and Coverdale, G.N., Two-Dimensional Monte Carlo Simulations to Capture Thick Chainlike Clusters of Ferromagnetic Particles in Colloidal Dispersions, *J. Colloid. Inter. Sci.*, 1996, 178, 620-627.

[10] Satoh, A., Chantrell, R.W., Kamiyama, S. and Coverdale, G.N., Three-Dimensional Monte Carlo Simulations of Thick Chainlike Clusters Composed of Ferromagnetic Fine Particles, *J. Colloid. Inter. Sci.*, 1996, 181, 422-428.

[11] Aoshima, M. and Satoh, A., Two-Dimensional Monte Carlo Simulations of a Polydisperse Colloidal Dispersion Composed of Ferromagnetic Particles for the Case of No External Magnetic Field, *J. Colloid. Inter. Sci.*, 2004, 280, 83-90.

[12] Aoshima, M. and Satoh, A., Two-Dimensional Monte Carlo Simulations of a Colloidal Dispersion Composed of Polydisperse Ferromagnetic Particles in an Applied Magnetic Field, *J. Colloid. Inter. Sci.*, 2005, 288, 475-488.

[13] Aoshima, M. and Satoh, A., Two-Dimensional Monte Carlo Simulations of a Colloidal Dispersion Composed of Rod-like Ferromagnetic Particles in the Absence of an Applied Magnetic Field, *J. Colloid. Inter. Sci.*, 2006, 293, 77-87.

[14] Aoshima, M. and Satoh, A., Two-Dimensional Monte Carlo Simulations of a Colloidal Dispersion Composed of Rod-like Ferromagnetic Particles in an Applied Magnetic Field, *Model. Simul. Mater. Sci. Eng.*, 2008, 16, 015004.

[15] Ozaki, M., Magnetic Properties of Hematite Suspensions, *Report of the Graduate School of Science ,Yokohama City University*, 1996, 47, 19-30. (in Japanese).

[16] Ishikawa, T. and Ozaki, M., Magnetic Properties of Hematite Micro-Particles in Aqueous Suspensions, in: *Proceedings of the 57th Divisional Meeting on Colloidal and Interface Chemistry*, the Chemical Society of Japan, 2004, 105. (in Japanese).

[17] Satoh, A., Ozaki, M., Ishikawa, T. and Majima, T., Transport Coefficients and Orientational Distributions of Rodlike Particles with Magnetic Moment Normal to the Particle Axis Under Circumstances of a Simple Shear Flow, *J. Colloid. Inter. Sci.*, 2005, 292, 581-590.

[18] Satoh, A. and Ozaki, M., Transport Coefficients and Orientational Distributions of a Magnetic Spheroidal Particles with a Magnetic Moment Normal to the Particle Axis (Analysis for an Applied Magnetic Field Normal to the Shear Plane, *J. Colloid. Inter. Sci.*, 2006, 298, 957-966.

[19] Satoh, A., *Introduction to Molecular-Microsimulation of Colloidal Dispersions*, Elsevier Science, Amsterdam, 2003.

[20] Satoh, A., *Monte Carlo Simulation*, Asakura Shoten, Tokyo, 1997. (in Japanese)

[21] Satoh, A., A New Technique for Metropolis Monte Carlo Simulation to Capture Aggregate Structures of Fine Particles: Cluster-Moving Monte Carlo Algorithm, *J. Colloid. Inter. Sci.*, 1992, 150, 461-472.